

Two- and Three-photon Fusion in Relativistic Heavy Ion Collisions

C.A. Bertulani^{a)}, and F. Navarra^{b)}

a) Department of Physics, Brookhaven National Laboratory, Upton, New York 11973-5000, USA

b) Instituto de Física, Universidade de São Paulo, C.P. 66318, 05315-970 São Paulo, SP, Brazil

The production of mesons in ultra-peripheral collisions of relativistic heavy ions is re-analyzed using a projection technique to calculate the amplitudes for the appropriate Feynman diagrams. The virtuality of the exchanged photons is fully accounted for in this approach. In the case of two-photon fusion, it is explicitly shown that the inclusion of nuclear form factors validates the equivalent photon approximation. However, this does not apply to three-photon fusion cross sections. The cross section of J/ψ production in ultra-peripheral collisions at RHIC and LHC are shown to be much smaller than the cross sections for the production of $C = \text{even}$ mesons of similar masses.

I. INTRODUCTION

Two-photon physics is the dominant process in e^+e^- colliders. This was first shown by Brodsky, Kinoshita and Terazawa [1]. In an earlier paper, Low [2] showed that one can relate the particle production by two real photons (with energies ω_1 and ω_2 , respectively) to the particle's decay width, $\Gamma_{\gamma\gamma}$. Since both processes involve the same matrix elements, only the phase-space factors and polarization summations are distinct. Low's formula is

$$\sigma(\omega_1, \omega_2) = 8\pi^2 \frac{\Gamma_{\gamma\gamma}}{M} \delta(4\omega_1\omega_2 - M^2), \quad (1)$$

where M is the particle mass, $\Gamma_{\gamma\gamma}$ its decay width, and the delta-function accounts for energy conservation.

Another important theoretical development was the realization that the cross sections in colliders are well described by replacing the virtual photons by an equivalent field of real photons. One often uses the concept of an equivalent photon number, $n(\omega)$, with energy ω . This approximation, called the Weizsäcker-Williams method [3] (or the equivalent photon approximation) yields for the particle production in colliders [1]

$$\sigma = \int d\omega_1 d\omega_2 \frac{n_1(\omega_1)}{\omega_1} \frac{n_2(\omega_2)}{\omega_2} \sigma_{\gamma\gamma}(\omega_1, \omega_2) \quad (2)$$

To our knowledge, ref. [4] was the first to apply a similar approach to study particle production in relativistic heavy ion collisions. As compared to e^+e^- colliders heavy ions carry the advantage of a larger coupling constant ($Z\alpha$), which increases the cross sections by a large factor. The disadvantage is that one needs to separate the final products from those created by strong interaction processes. Inserting eq. 1 in 2 and using the equivalent photon numbers appropriate to heavy ions the following expression was obtained in ref. [4], to leading logarithmic order,

$$\sigma = \frac{128}{3} Z^4 \alpha^2 \frac{\Gamma_{\gamma\gamma}}{M^3} \ln^3 \left(\frac{2\gamma\delta}{MR} \right), \quad (3)$$

where $\delta = 0.681\dots$, γ is the Lorentz factor (e.g., $\gamma = 108$ for the RHIC collider at Brookhaven), and R is a parameter which depends on the mass of the produced particle. If M is much smaller than the inverse of a typical nuclear radius, then $R = 1/M$, otherwise R is the nuclear radius. These choices reflect the uncertainty relation in the direction transverse to the beam, as explained in ref. [4]. Since spin 1 particles cannot couple to two real photons [5], one expects that only spin 0 and spin 2 particles are produced.

Following these ideas, the two-photon fusion mechanism in heavy ion collisions was exploited by several authors, including the possibility to search for the Higgs boson [6–13]. At present, there are experiments at RHIC/Brookhaven, and proposed ones for the Large Hadron Collider at CERN (LHC) [14], which aim to study these phenomena. For mesons the cross section is very sensitive to the minimum impact parameter, and refs. [9,10] have shown that corrections to eq. 3 are substantial. These corrections are of geometrical nature and use the equivalent photon method, as in eq. 3.

Due to the large theoretical and experimental interest in these phenomena [6–14] (see also ref. [15] and references therein), it is important to calculate the production mechanism with an alternative approach. We use the projection

method of ref. [16] to obtain the meson-production amplitude in terms of the amplitude for production of quark-anti-quark pairs by the time-dependent field of the colliding nuclei. In section 2 we start with a calculation for the production of parapositronium in heavy ions colliders. This will define the calculational steps we need for the production of mesons. In particular, we show that the results agree with a recent calculation for this process [17], thus validating the projection method. In section 3 we extend the calculation to the production of $C = \text{even}$ mesons. In this case, one has to account for the nuclear form factors. We show that the equivalent photon method is obtained as a consequence of the cutoff of large photon momenta, imposed by the inclusion of the nuclear form factors. In section 4 we calculate the cross section for the production of vector mesons ($C = \text{odd}$) by three-virtual photons. In particular, we show that the production rates for J/ψ mesons are many orders of magnitude smaller than for the $C = \text{even}$ mesons of similar masses.

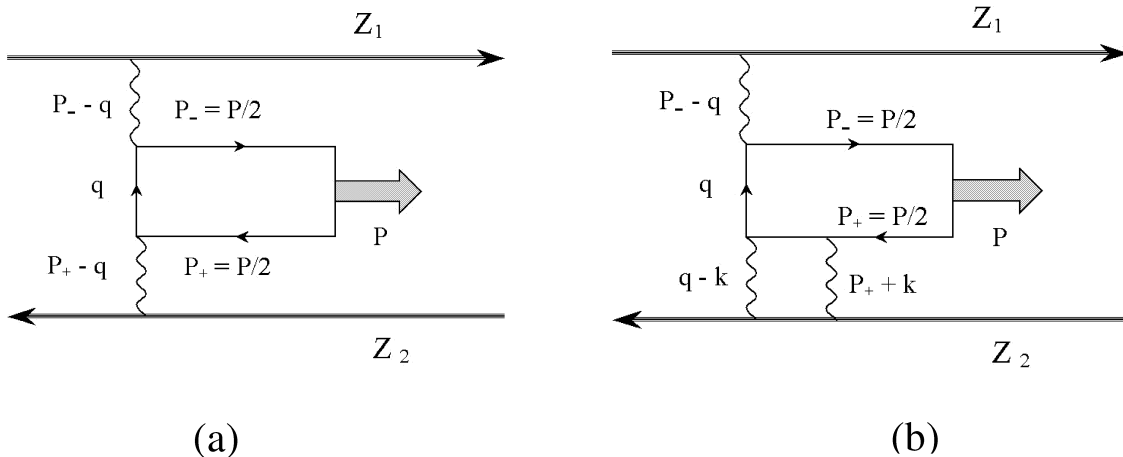


FIG. 1. Feynman graphs for two- and three-photon fusion in ultra-peripheral collisions of relativistic heavy ions.

II. TWO-PHOTON FUSION IN HEAVY ION COLLIDERS

In the laboratory frame the Fourier components of the classical electromagnetic field at a distance $\mathbf{b}/2$ of nucleus 1 with charge Ze and velocity β , is given by (in our notation $q = (q_0, \mathbf{q}_t, q_3)$, and $q_3 \equiv q_z$)

$$A_0^{(1)}(q) = -8\pi^2 Ze \delta(q_0 - \beta q_3) \frac{e^{i\mathbf{q}_t \cdot \mathbf{b}/2}}{q_t^2 + q_3^2/\gamma^2} \quad \text{and} \quad A_3^{(1)} = \beta A_0^{(1)} \quad (4)$$

For the field of nucleus 2, moving in the opposite direction, we replace β by $-\beta$ and \mathbf{b} by $-\mathbf{b}$ in the equations above. Although $\beta \simeq 1$ in relativistic colliders, it is important to keep them in the key places, as some of their combinations will lead to important $\gamma = (1 - \beta^2)^{-1/2}$ factors.

The matrix element for the production of positronium is directly obtained from the corresponding matrix element for the production of a free pair (see fig. 1(a)), with the requirement that $P_+ = P_- = P/2$, where P is the momentum of the final bound state. That is

$$\begin{aligned} \mathcal{M} &= \mathcal{M}_1 + \mathcal{M}_2 \\ &= -ie^2 \bar{u}\left(\frac{P}{2}\right) \left[\int \frac{d^4 q}{(2\pi)^4} \mathcal{A}^{(1)}\left(\frac{P}{2} - q\right) \frac{\not{q} + M/2}{q^2 - M^2/4} \mathcal{A}^{(2)}\left(\frac{P}{2} + q\right) + \mathcal{A}^{(1)}\left(\frac{P}{2} + q\right) \frac{\not{q} + M/2}{q^2 - M^2/4} \mathcal{A}^{(2)}\left(\frac{P}{2} - q\right) \right] v\left(\frac{P}{2}\right), \quad (5) \end{aligned}$$

where M is the positronium mass.

The treatment of bound states in quantum field theory is a very complex subject (for reviews, see [18]). In our case, we want to use the matrix element for free-pair production and relate the results for the production of a bound-pair. A common trick used in this situation is to convolute the matrix element given above with the bound-state wave function. One can show (see, e.g., [16]) that this is equivalent to the use of a projection operator of the form

$$\bar{u} \cdots v \longrightarrow \frac{\Psi(0)}{2\sqrt{M}} \text{tr} [\cdots (\not{P} + M) i \gamma^5] \quad \text{and} \quad \bar{u} \cdots v \longrightarrow \frac{\Psi(0)}{2\sqrt{M}} \text{tr} [\cdots (\not{P} + M) i \not{\hat{e}}^*] \quad (6)$$

where \cdots is any matrix operator. The first equation applies to a spin 0 (parapositronium) and the second to spin 1 (orthopositronium) particles, respectively. In these equations $\Psi(\mathbf{r})$ is the bound state wavefunction calculated at the origin, and \hat{e}^* is the polarization vector, given by $\hat{e}_{\pm 1}^* = (0, 1/\sqrt{2}, \pm i/\sqrt{2}, 0)$ and $\hat{e}_0^* = (0, 0, 0, 1)$.

Using eq. 6 in eq. 5, one gets for the parapositronium production

$$\begin{aligned} \mathcal{M}_1 = & 4ie^2 \frac{\Psi(0)}{2\sqrt{M}} \int \frac{d^4q}{(2\pi)^4} \frac{1}{q^2 - M^2/4} \left[\epsilon_{0\mu 3\nu} P_\nu q_\mu A_0^{(1)}(P/2 - q) A_3^{(2)}(P/2 + q) \right. \\ & \left. + \epsilon_{3\mu 0\nu} P_\nu q_\mu A_3^{(1)}(P/2 - q) A_0^{(2)}(P/2 + q) \right], \end{aligned} \quad (7)$$

where $\epsilon_{\lambda\mu\nu\sigma}$ is the antisymmetric Levi-Civita tensor.

Inserting the explicit form of the electromagnetic fields in eq. 7 we get

$$\mathcal{M}_1 = ie^2 \frac{\Psi(0)}{\sqrt{M}} \frac{2}{(2\pi)^4} [\epsilon_{0\mu 3\nu} P_\nu J_{0\mu 3} + \epsilon_{3\mu 0\nu} P_\nu J_{3\mu 0}], \quad (8)$$

where

$$\begin{aligned} J_{0\mu 3} = & (8\pi^2 Z e)^2 \beta \int \frac{d^4q}{q^2 - M^2/4} q_\mu \delta[(P/2 - q)_0 - \beta(P/2 - q)_z] \delta[(P/2 + q)_0 + \beta(P/2 + q)_z] \\ & \times \frac{\exp[i(\mathbf{P}_t/2 - \mathbf{q}_t) \cdot \mathbf{b}/2]}{\left[(\mathbf{P}_t/2 - \mathbf{q}_t)^2 + (P_z/2 - q_z)^2/\gamma^2 \right]} \frac{\exp[-i(\mathbf{P}_t/2 + \mathbf{q}_t) \cdot \mathbf{b}/2]}{\left[(\mathbf{P}_t/2 + \mathbf{q}_t)^2 + (P_z/2 + q_z)^2/\gamma^2 \right]}. \end{aligned} \quad (9)$$

The delta functions imply the conditions

$$q_z = -P_0/2\beta \quad \text{and} \quad q_0 = -\beta P_z/2. \quad (10)$$

We also note that $J_{0\mu 3} = -J_{3\mu 0}$ and $\epsilon_{0\mu 3\nu} = \epsilon_{3\mu 0\nu}$, and also that \mathcal{M}_2 , which is obtained by the replacement $A^{(1)} \leftrightarrow A^{(2)}$ in \mathcal{M}_1 , is the same as \mathcal{M}_1 , i.e., $\mathcal{M}_1 = \mathcal{M}_2$. In other words, the direct (fig. 1(a)) and the exchange Feynman diagrams yield the same result for the matrix element. This is a consequence of the imposed condition that $P_- = P_+ = P/2$ and of the projection onto the bound-state. It is an important result that will also show up in the diagrams involving three-photons. Gathering all these results, and using $\epsilon_{0\mu 3\nu} P_\nu J_\mu = |\mathbf{P} \times \mathbf{I}|$, we get

$$\mathcal{M} = 16i \frac{\Psi(0)}{\sqrt{M}} (Z\alpha)^2 |\mathbf{P} \times \mathbf{I}|, \quad (11)$$

where

$$\mathbf{I} = \int \frac{d^2q_t \mathbf{q}_t}{q_t^2 + Q^2} \frac{1}{\left[(\mathbf{P}_t/2 + \mathbf{q}_t)^2 + \omega_1^2/\gamma^2 \right]} \frac{1}{\left[(\mathbf{P}_t/2 - \mathbf{q}_t)^2 + \omega_2^2/\gamma^2 \right]}, \quad (12)$$

with

$$Q^2 = \frac{M^2}{2} + \frac{P_t^2}{4} + \frac{P_z^2}{2\gamma^2} \simeq \frac{M^2}{2} + \frac{P_t^2}{4} \quad (13)$$

and

$$\omega_1 = \frac{E/\beta - P_z}{2}, \quad \omega_2 = \frac{E/\beta + P_z}{2} \quad \text{and} \quad 4\omega_1\omega_2 = M^2 + P_t^2 - P_z/\gamma^2 \simeq M^2 + P_t^2, \quad (14)$$

where $E \equiv P_0$ is the total positronium energy.

We see that ω_1 and ω_2 play the role of the (real) photon energies. For real photons one expects $4\omega_1\omega_2 = E^2$, as in eq. 1.

The two-photon fusion cross sections can be obtained by using

$$d\sigma = \sum_\mu \left[\int d^2b |\mathcal{M}(\mu)|^2 \right] \frac{d^3P}{(2\pi)^3 2E} \quad (15)$$

Since the important impact parameters for the production of the positronium will be $b > 1/m_e \gg R$, where R is the nuclear radius, the integral over impact parameter can start from $b = 0$. Thus, the integral over impact parameter in eq. 15 yields the delta function

$$\frac{1}{(2\pi)^2} \int \exp[i(\mathbf{q}_t - \mathbf{q}'_t) \cdot \mathbf{b}] d^2b = \delta(\mathbf{q}_t - \mathbf{q}'_t) . \quad (16)$$

We thus obtain

$$\frac{d\sigma}{d^3P} = \frac{64}{\pi ME} \left| \Psi(0) \right|^2 (Z\alpha)^4 \int \frac{d^2q_t}{(q_t^2 + Q^2)^2} \frac{(\mathbf{P}_t \times \mathbf{q}_t)^2}{\left[(\mathbf{P}_t/2 + \mathbf{q}_t)^2 + \omega_1^2/\gamma^2 \right]^2} \frac{1}{\left[(\mathbf{P}_t/2 - \mathbf{q}_t)^2 + \omega_2^2/\gamma^2 \right]^2} . \quad (17)$$

We now show that the above equation is equal to the equation obtained in ref. [17]. First we change the variables to

$$\mathbf{q}_{1t} = \frac{\mathbf{P}_t}{2} - \mathbf{q}_t , \quad \mathbf{q}_{2t} = \frac{\mathbf{P}_t}{2} + \mathbf{q}_t , \quad q_{1z} = \frac{P_z/2 - q_z}{\gamma} , \quad q_{2z} = \frac{P_z/2 + q_z}{\gamma} . \quad (18)$$

It is easy to show that

$$(\mathbf{P}_t/2 - \mathbf{q}_t)^2 + \omega_2^2/\gamma^2 = q_{1t}^2 + q_{1z}^2 = -q_1^2 , \quad \text{and} \quad (\mathbf{P}_t/2 + \mathbf{q}_t)^2 + \omega_1^2/\gamma^2 = q_{2t}^2 + q_{2z}^2 = -q_2^2 , \quad (19)$$

and that

$$\mathbf{P}_t \times \mathbf{q}_t = \mathbf{q}_{1t} \times \mathbf{q}_{2t} , \quad \text{and} \quad q_t^2 + Q^2 \simeq q_t^2 - \frac{M^2}{2} + \frac{P_t^2}{4} = q_1^2 + q_2^2 - M^2 \quad (20)$$

The positronium wavefunction at the origin is very well known. It is given by $\left| \Psi(0) \right|^2 = M^3 \alpha^3 / 64\pi$, where M is the positronium mass. Thus, eq. 17 becomes

$$E \frac{d\sigma}{d^3P} = \frac{\zeta(3)}{\pi} \frac{\sigma_0}{M^2} J_B , \quad (21)$$

where

$$J_B = \frac{M^2}{\pi} \int \mathbf{A}^2 \delta(\mathbf{q}_{1t} + \mathbf{q}_{2t} - \mathbf{P}_t) d\mathbf{q}_{1t} d\mathbf{q}_{2t} , \quad (22)$$

with

$$\mathbf{A} = \frac{\mathbf{q}_{1t} \times \mathbf{q}_{2t}}{q_1^2 q_2^2} \frac{M^2}{M^2 - q_1^2 - q_2^2} , \quad \zeta(3) = 1.202\dots , \quad \text{and} \quad \sigma_0 = \frac{4Z^4 \alpha^7}{M^2} . \quad (23)$$

We have included the zeta-function $\zeta(3)$ to take into account the production of the para-positronium in higher orbits, besides the production in the K-shell.

The equation 21 is exactly the same as eq. 2.23 of ref. [17]. Thus we have shown that the approach used in this article for the production of a bound particle (in this case, the para-positronium) by means of the two-photon fusion yields the same results as in the approach of ref. [17]. In that article the total cross section for the production of the para-positronium was obtained by separating the regions where a leading order logarithmic approximation could be used and a region where the integral in eq. 22 could be solved numerically. To verify their results we will follow a different route. Using eq. 17 we can do the integration over the angle ϕ between \mathbf{P}_t and \mathbf{q}_t analytically. We get

$$\sigma = \frac{M^4}{2\pi} \zeta(3) \sigma_0 \int dP_t dP_z dq_t \frac{q_t^3 P_t^3}{E} \frac{N(q_t, P_t, P_z)}{(q_t^2 + Q^2)^2} , \quad (24)$$

where

$$N(q_t, P_t, P_z) = \frac{2\pi}{b^4} \frac{\sqrt{a_2^2 - 1}(a_1^2 - a_1 a_2 - 2) + \sqrt{a_1^2 - 1}(a_2^2 - a_1 a_2 - 2)}{\sqrt{a_1^2 - 1} \sqrt{a_2^2 - 1} (a_1 + a_2)^3} , \quad (25)$$

where

$$b = q_t P_t , \quad a_1 = \frac{P_t^2/4 + q_t^2 + \omega_1^2/\gamma^2}{q_t P_t} \quad \text{and} \quad a_2 = \frac{P_t^2/4 + q_t^2 + \omega_2^2/\gamma^2}{q_t P_t} . \quad (26)$$

The triple integral in eq. 24 can be calculated numerically. For RHIC, using $\gamma = 108$ and $Au + Au$ collisions, we find $\sigma = 19.4$ mb. For the LHC, using $\gamma = 3000$ and $Pb + Pb$ collisions, we find $\sigma = 116$ mb. These are in good agreement with the results of ref. [17].

III. PRODUCTION OF $C = \text{EVEN}$ MESONS

We can extend the calculation of the previous section to account for the production of mesons with spin $J = 0$ and $J = 2$ by the two-photon fusion mechanism. The following procedure is to be adopted:

1. Replace the electron-positron lines by quark-antiquarks in the diagram of figure 1(a).
2. M in the following formulas will refer to the meson mass.
3. Replace α^2 by $\alpha^2 (2J + 1) 3 \sum_i Q_i^4$, where 3 accounts for the number of colors, and Q_i is the fractional quark charge.

These two last factors will cancel out when we express $|\Psi(0)|^2$ in terms of $\Gamma_{\gamma\gamma}$, the decay-width of the meson. To understand how this is done, let's discuss the basics of the annihilation process of a positronium (see also ref. [21]). With probability α^2 the e^- can fluctuate and emit a virtual photon with energy m_e . The electron recoils and can travel up to a distance $\sim 1/m_e$ (or time $\sim m_e$) to meet the positron and annihilate. This occurs when e^- and e^+ are both found close together in a volume of size $(1/m_e)^3$, i.e., with a probability given by $|\Psi(0)|^2/m_e^3$. Thus, the annihilation probability per unit time (decay width) is $\Gamma \sim \alpha^2 |\Psi(0)|^2/m_e^2$. Angular momentum conservation and CP invariance does not allow the ortho-positronium to decay into an even number of photons [5]. The description of the annihilation process given above is thus only appropriate for the para-positronium. A detailed QED calculation yields an extra 4π in the formula above. This yields $\Gamma_{\gamma\gamma}(^1S_0) = 8.03 \times 10^9 \text{ s}^{-1}$, while the experimental value [22] is $7.99(11) \times 10^9 \text{ s}^{-1}$, in good agreement with the theory. For mesons, including the color and the charge factors, as described before, the relationship between $\Psi(0)$ and $\Gamma_{\gamma\gamma}$ arise due to the same reasons. One gets $\Gamma_{\gamma\gamma} = 16\pi\alpha^2 |\Psi(0)|^2 / M^2 \cdot 3 \sum_i Q_i^4$.

According to these arguments the connection between $\Gamma_{\gamma\gamma}$ and $|\Psi(0)|^2$, extended to meson decays, should be valid for large quark masses so that $1/m_q \ll \sqrt{\langle r^2 \rangle}$, where $\sqrt{\langle r^2 \rangle}$ is the mean size of the meson. Thus, it should work well for, e.g. charmonium states, $c\bar{c}$. In fact, Appelquist and Politzer [24] have generalized this derivation for the hadronic decay of heavy quark states, which besides other phase-space considerations amounts in changing α to α_s , the strong coupling constant. This can be simply viewed as a way to get a constraint on the wavefunction $|\Psi(0)|^2$ [23]. One expects that these arguments are valid to zeroth order in quantum chromodynamics and in addition one should include relativistic corrections. But, as shown in [21], the inclusion of relativistic effects, summing diagrams to higher order in the perturbation series, is equivalent to solving the non-relativistic Schrödinger equation.

4. Change the integration variable to \mathbf{q}_{1t} and \mathbf{q}_{2t} .
5. Introduce form factors $F(q_{1t})$ and $F(q_{2t})$ to account for the nuclear dimensions. This is a simple way to eliminate the integral over impact parameters and will be justified 'a posteriori', i.e., when we compare our results with those from other methods. These form factors will impose a cutoff in q_{1t} and q_{2t} , so that

$$q_{1t}, q_{2t} \simeq \frac{1}{R} \ll M, \quad (27)$$

where R is a typical nuclear size. Taking $R = 6.5 \text{ fm}$, we get $1/R \sim 30 \text{ MeV}$. This is much smaller than the meson masses. As an outcome of this condition, we can replace $Q^2 \sim M^2/2$ in eq. 13.

According the procedures 1-5 we get from eq. 17,

$$\frac{d\sigma}{dP_z} = \frac{16(2J+1)}{\pi^2} \frac{Z^4 \alpha^2}{M^3} \Gamma_{\gamma\gamma} \frac{1}{E} \int d\mathbf{q}_{1t} d\mathbf{q}_{2t} (\mathbf{q}_{1t} \times \mathbf{q}_{2t})^2 \frac{[F_1(q_{1t}^2) F_2(q_{2t}^2)]^2}{(q_{1t}^2 + \omega_1^2/\gamma^2)^2 (q_{2t}^2 + \omega_2^2/\gamma^2)^2} \quad (28)$$

Using eqs. 14 we have

$$E = \omega_1 + \omega_2, \quad \omega_1 - \omega_2 = P_z, \quad \text{and} \quad \omega_1 \omega_2 = M^2/4$$

so that

$$dP_z = \left(1 + \frac{M^2}{4\omega_1^2}\right) d\omega_1, \quad \text{and} \quad E = \frac{\omega_1^2 + M^2/4}{\omega_1}. \quad (29)$$

Thus,

$$\frac{d\sigma}{d\omega_1} = \sigma^{(+)} \frac{d\mathcal{N}_{2\gamma}(\omega_1)}{d\omega_1} = \sigma^{(+)} \frac{1}{\omega_1} n_1(\omega_1)n_2(\omega_2), \quad (30)$$

where

$$\sigma^{(+)} = 8\pi^2(2J+1)\frac{\Gamma_{\gamma\gamma}}{M^3} \quad \text{and} \quad n_i(\omega_i) = \frac{2}{\pi} Z^2\alpha \int \frac{dq q^3 [F_i(q^2)]^2}{(q^2 + \omega_i^2/\gamma^2)^2}. \quad (31)$$

We notice that $n(\omega)$ is the frequently used form of the equivalent photon number which enters eq. 2. Thus, eqs. 30 and 31 are the result one expects by using the equivalent photon method, i.e., by using eqs. 1 and 2. This is an important result, since it shows that the projection method to calculate the two-photon production of mesons works even for light quark masses (i.e., for π^0). In this case there seems to be no justification for replacing the quark masses and momenta by half the meson masses and momenta, as we did for the derivation of eq. 28. This looks quite intriguing, but it is easy to see that the step 3 in our list of procedures adopted is solely dependent on the meson mass, not on the quark masses, i.e., if they are constituent, sea quarks, etc. Moreover, the projection method eliminates the reference to quark masses in the momentum integrals. The condition 27 finishes the job, by eliminating the photon virtualities and yielding the same result one would get with the equivalent photon approximation.

In the next section we will extend this approach to the calculation of vector meson ($J = 1^-$) production by three photons. There we will also apply the results to light quark masses, but we will not be able to check the results against the equivalent photon method since we cannot calculate the process as originating from the collisions of three real photons.

We now define a ‘‘two-photon equivalent number’’, $\mathcal{N}_{2\gamma}(M^2)$, so that $\sigma = \sigma^{(+)}\mathcal{N}_{2\gamma}(M^2)$, where

$$\mathcal{N}_{2\gamma}(M^2) = \int d\omega \frac{d\mathcal{N}_{2\gamma}}{d\omega} = \int \frac{d\omega}{\omega} n_1(\omega) n_2\left(\frac{M^2}{4\omega}\right). \quad (32)$$

To calculate this integral we need the equivalent photon numbers given by eq. 31. The simplest form factor one can use for this purpose is the ‘sharp-cutoff’ model, which assumes that

$$F(q^2) = 1 \text{ for } q^2 < 1/R, \quad \text{and } F(q^2) = 0, \text{ otherwise.} \quad (33)$$

In this case, we can use the integral

$$\int_0^{1/R} \frac{dq q^3}{(q^2 + \omega^2/\gamma^2)^2} = \frac{1}{2} \left[\ln\left(1 + \frac{\gamma^2}{\omega^2 R^2}\right) - \frac{1}{1 + \omega^2 R^2/\gamma^2} \right], \quad (34)$$

and get for the differential cross section

$$\frac{d\sigma}{d\omega} = \sigma^{(+)} \frac{Z^4\alpha^2}{\pi^2\omega} \left[\ln\left(1 + \frac{\gamma^2}{\omega^2 R^2}\right) - \frac{1}{1 + \omega^2 R^2/\gamma^2} \right] \left[\ln\left(1 + \frac{16\gamma^2\omega^2}{M^4 R^2}\right) - \frac{1}{1 + M^4 R^2/16\gamma^2\omega^2} \right]. \quad (35)$$

The spectrum possesses a characteristic $1/\omega$ dependence, except for $\omega \gg \gamma/R$, when it decreases as $1/\omega^5$.

When the condition $\gamma \gg MR$ is met, we can neglect the unity factors inside the logarithm in eq. 34, as well as the second term inside brackets. Then, doing the integration of 35 from $\omega = M^2 R/4/\gamma$ to $\omega = \gamma/R$, we get eq. 3. But, eq. 35 is an improvement over eq. 3. Eq. 3 is often used in the literature, but it is only valid for $\gamma \gg MR$. This relation does not apply to, e.g., the Higgs boson production ($M_{H^0} \sim 100$ GeV), as considered in ref. [6].

For quantitative predictions we should use a more realistic form factor. The Woods-Saxon distribution, with central density ρ_0 , size R , and diffuseness a gives a good description of the densities of the nuclei involved in the calculation. However, this distribution is very well described by the convolution of a hard sphere and an Yukawa function [25]. In this case, the form factors can be calculated analytically

$$F(q^2) = \frac{4\pi\rho_0}{q^3} [\sin(qR) - qR \cos(qR)] \left[\frac{1}{1 + q^2 a^2} \right]. \quad (36)$$

For Au we use $R = 6.38$ fm, and $a = 0.535$ fm, with ρ_0 normalized so that $\int d^3r \rho(r) = 197$. For Pb the appropriate numbers are 6.63 fm, 0.549 fm, and 208, respectively [19]. With this form factor the two-photon equivalent photon number $d\mathcal{N}_{2\gamma}/d\omega$ is also obtainable in a closed form. In table 1 we show the cross sections for the production of $C = \text{even}$ mesons at RHIC ($Au + Au$) and LHC ($Pb + Pb$) using the formalism described above.

Table 1. Cross sections for two-photon production of ($C = \text{even}$) mesons at RHIC ($Au + Au$) and at LHC ($Pb + Pb$).

meson	mass [MeV]	$\Gamma_{\gamma\gamma}$ [keV]	$\sigma^{(+)}$ [nb]	$\mathcal{N}_{2\gamma}^{RHIC}/10^3$	$\mathcal{N}_{2\gamma}^{LHC}/10^7$	σ^{RHIC} [μb]	σ^{LHC} [mb]
π_0	134	7.8×10^{-3}	99	49	2.8	4940	28
η	547	0.46	86	12	1.8	1000	16
η'	958	4.2	147	5.1	1.4	746	21
$f_2(1270)$	1275	2.4	179	3.0	1.2	544	22
$a_2(1320)$	1318	1.0	67	2.9	1.1	195	8.2
η_c	2981	7.5	8.7	0.38	0.7	3.3	0.61
χ_{0c}	3415	3.3	2.6	0.24	0.63	0.63	0.16
χ_{2c}	3556	0.8	2.8	0.21	0.56	0.59	0.15

As pointed out in refs. [9,10], one can improve the (classical) calculation of the two-photon luminosities by introducing a geometrical factor (the Θ -function in ref. [9]), which affects the angular part of the integration over impact parameters. This factor takes care of the position where the meson is produced in the space surrounding the nuclei. In our approach the form factors also introduce a geometrical cutoff implying that the mesons cannot be produced inside the nuclei. However, it is not easy to compare both approaches directly, as we obtain a momentum representation of the amplitudes when we perform the integration over impact parameters to obtain eq. 28. But we can compare the effects of geometry in both cases by using equation 35. After performing the integral over ω , we can rewrite it as

$$\sigma = \int ds \mathcal{L}(s) \sigma_{\gamma\gamma}(s), \quad (37)$$

where $s = 4\omega_1\omega_2$ is the square of the center-of-mass energy of the two photons, $\sigma(s)$ is given by eq. 1, and $\mathcal{L}(s)$ is the “photon-photon luminosity”, given by

$$\mathcal{L}(s) = \frac{1}{s} \frac{Z^4 \alpha^2}{\pi^2} \int \frac{d\omega}{\omega} \left[\ln \left(1 + \frac{\gamma^2}{\omega^2 R^2} \right) - \frac{1}{1 + \omega^2 R^2 / \gamma^2} \right] \left[\ln \left(1 + \frac{16\gamma^2 \omega^2}{s^2 R^2} \right) - \frac{1}{1 + s^2 R^2 / 16\gamma^2 \omega^2} \right]. \quad (38)$$

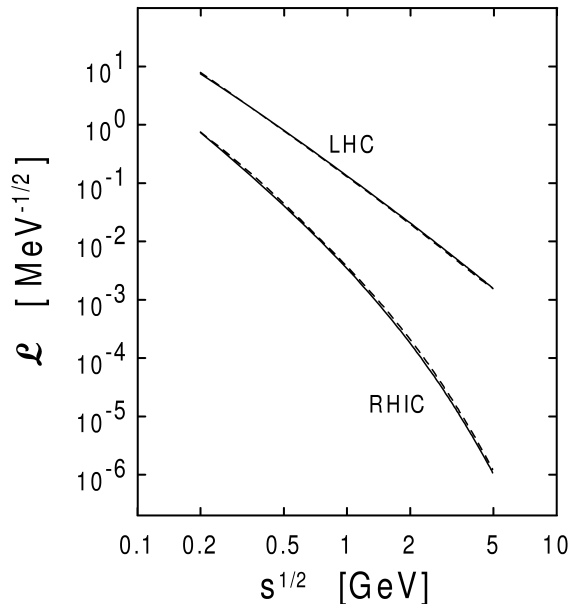


FIG. 2. Two-photon luminosities (see definition in eq. 37) at RHIC and LHC. Dashed lines include a geometric correction.

In figure 2 we compare the result obtained by eq. 38 and that of ref. [9]. The luminosities for RHIC ($Au + Au$) and for LHC ($Pb + Pb$) are presented. For RHIC the difference between the two results can reach 10% for very large meson masses (e.g. the Higgs), but we notice that for the LHC the two results are practically identical, the difference being of the order of 3%, or less, even for the Higgs. Thus, the improved version of eq. 3, given by integrating eq. 35, is accurate enough to describe meson production by two-photon fusion. Other effects, like the interference between the electromagnetic and the strong interaction production mechanism in grazing collisions, must yield larger corrections to the (non-disruptive) meson production cross sections than a more elaborate description of geometrical effects.

The results in this section are very important for our purpose of calculating the production of vector mesons by means of three-photon fusion in peripheral collisions. This could be a relevant process, e.g., for a study of the three-photon-vertex in charmonium production.

One might think that the calculation could be performed by using the equivalent photon approximation that, as we have seen in this section, works so well for $C = \text{even}$ mesons. However, the introduction of a third photon leads to an additional integration, which implies that at least two of the exchanged photons cannot be treated as real ones. Nonetheless, the results of this section paves the way to the calculation of production of $C = \text{odd}$ mesons. Although the use of the projection technique to systems composed of light quarks is questionable, we have seen that it works, basically because of the relation 27, due to the inclusion of the nuclear form-factors.

IV. PRODUCTION OF VECTOR MESONS

Lets now consider the diagram of figure 1(b), appropriate for the fusion of three photons into a $C = \text{odd}$ particle. According to the Feynman rules, the matrix element for it is given by

$$\mathcal{M}_a = e^3 \bar{u}\left(\frac{P}{2}\right) \int \frac{d^4 q}{(2\pi)^4} \int \frac{d^4 k}{(2\pi)^4} \mathcal{A}^{(1)}\left(\frac{P}{2} - q\right) \frac{\not{q} + M/2}{q^2 - M^2/4} \mathcal{A}^{(2)}(q - k) \frac{\not{k} + M/2}{k^2 - M^2/4} \mathcal{A}^{(2)}\left(\frac{P}{2} + k\right) v\left(\frac{P}{2}\right). \quad (39)$$

There will be 12 diagrams like this. But, as we will see below, the upper photon leg in diagram of fig. 1(b) can be treated as a real photon, meaning that the equivalent photon approximation is valid for this piece of the diagram.

One has to use the second of the eqs. 6 to account for the projection onto $C = \text{odd}$ particles. The calculation of the traces is quite lengthy and was performed using the program FORM [26]. We have found out that the particle is produced with its polarization vector in the transverse direction, as the coefficients accompanying \hat{e}_0^* are of higher order in $1/\gamma$. Neglecting such terms we get

$$\begin{aligned} & A_\alpha^{(1)} A_\beta^{(2)} A_\lambda^{(2)} \text{Tr}[\gamma^\alpha (\gamma^\mu q_\mu + M/2) \gamma^\beta (\gamma^\nu k_\nu + M/2) \gamma^\lambda (\gamma^\rho P_\rho + M) \hat{e}_\eta^* \gamma^\eta] \\ &= -16 M A_0^{(1)} A_0^{(2)} A_0^{(2)} (k_0 + \beta k_3) (\mathbf{q}_t - \mathbf{P}_t/2) \cdot \hat{\mathbf{e}}^*. \end{aligned} \quad (40)$$

The above product of the longitudinal components of A_μ yields factors proportional to the delta-function, i.e.,

$$A_0^{(1)} A_0^{(2)} A_0^{(2)} \propto \delta\left[\frac{E}{2} - q_0 - \beta\left(\frac{P_3}{2} - q_3\right)\right] \delta[q_0 - k_0 + \beta(q_3 - k_3)] \delta\left[\frac{E}{2} + k_0 - \beta\left(\frac{P_3}{2} + k_3\right)\right]. \quad (41)$$

These delta-functions lead to the conditions

$$q_3 = -\frac{E}{2\beta}, \quad q_0 = -\frac{P_3\beta}{2}, \quad \text{and} \quad k_0 = -\beta k_3 - \beta\omega_2, \quad (42)$$

where ω_2 is given by 14.

The integral over q_0 , k_0 and k_3 yields a factor $1/2$, and the matrix element becomes

$$\begin{aligned} \mathcal{M}_a &= \frac{8}{\pi^2} (Z\alpha)^3 \sqrt{M} \Psi(0) \int d^2 q_t d^3 k \frac{(\mathbf{q}_t - \mathbf{P}_t/2) \cdot \hat{\mathbf{e}}^*}{q^2 - M^2/4} \frac{\omega_2}{k^2 - M^2/4} \left[(\mathbf{P}_t/2 - \mathbf{q}_t)^2 + \omega_2^2/\gamma^2 \right]^{-1} \\ &\times \left[(\mathbf{q}_t - \mathbf{k}_t)^2 + (E/2\beta + k_3)^2/\gamma^2 \right]^{-1} \left[(\mathbf{P}_t/2 + \mathbf{k}_t)^2 + (P_3/2 + k_3)^2/\gamma^2 \right]^{-1} \exp(\mathbf{q}_t \cdot \mathbf{b}/2) \end{aligned} \quad (43)$$

As in eq. 17 we know that the nuclear form factors imply

$$q_t, \quad P_t, \quad k_t \simeq \frac{1}{R} \ll M, \quad (44)$$

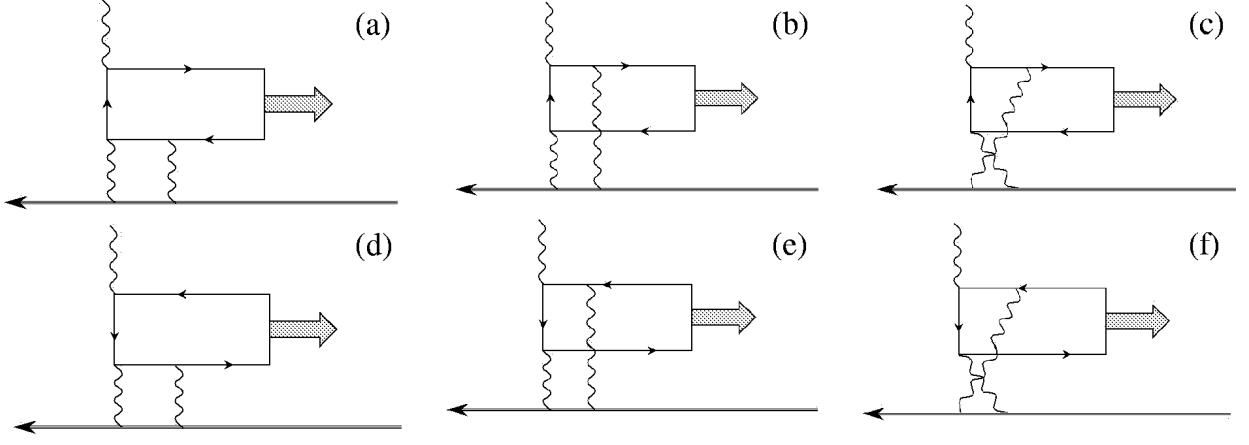


FIG. 3. Feynman graphs for three-photon fusion in ultra-peripheral collisions of relativistic heavy ions.

We can thus use the approximation for the propagator $(q^2 - M^2/4)^{-1} \simeq -2/M^2$. Changing the integration variable from \mathbf{k} to $\mathbf{k}' = \mathbf{k} + \mathbf{P}/2$, the propagators in the second line of 43 become

$$\left[(\mathbf{q}_t + \mathbf{P}_t/2 - \mathbf{k}'_t)^2 + (\beta E/2 - P_3/2 + k'_3)^2 / \gamma^2 \right]^{-1} \left[k_t'^2 + k_3'^2 / \gamma^2 \right]^{-2} \quad (45)$$

The integrand peaks sharply at $\mathbf{k}'_t = 0$ and one can eliminate \mathbf{k}'_t from the first term inside brackets.

Thus, the matrix element 43 becomes

$$\begin{aligned} \mathcal{M}_a = & -\frac{16}{\pi} (Z\alpha)^3 \frac{\Psi(0)}{M^{3/2}} \int d^2 q_t dk_t k_t \frac{(\mathbf{q}_{1t} \cdot \mathbf{e}^*) \exp(\mathbf{q}_t \cdot \mathbf{b}/2)}{[q_{1t}^2 + \omega_2^2 / \gamma^2]} \\ & \times \int dk_3 [k_t^2 + k_3^2 / \gamma^2]^{-1} [q_{2t}^2 + (\omega_1 + k_3)^2 / \gamma^2]^{-1} [k_3 + \omega_2 - \omega_1 - k_3^2 / 2\omega_2 \gamma^2]^{-1} \end{aligned} \quad (46)$$

where \mathbf{q}_{1t} and \mathbf{q}_{2t} are defined in eqs. 18 and ω_1 and ω_2 are defined in eq. 14.

If this matrix element was the only one being considered it would be easy to show that the one-photon exchange with one of the nuclei can be treated in the equivalent photon approximation. This arises from the structure of the first term inside the integral in 46. This result was expected in view of our results of the last section. But, the two-photon exchange in the lower part of the diagram leads to complicated integrals which cannot be simplified in terms of equivalent photons.

We thus need to calculate the six diagrams which are obtained by interchange of the two-photon lines, as shown in figure 3, and multiply the result by 2 to account for the same set of diagrams by inverting the roles of each nucleus. We calculate the amplitudes related to the diagrams by means of the same procedures we adopted in eqs. 39 through 46. We find that the matrix elements for the diagrams (b), (c), (e) and (f) of figure 2 are by a factor $1/\gamma$ smaller than those for the diagrams (a) and (d). The amplitude for the diagram (d) in figure 2 yields

$$\begin{aligned} \mathcal{M}_d = & -\frac{16}{\pi} (Z\alpha)^3 \frac{\Psi(0)}{M^{3/2}} \int d^2 q_t dk_t k_t \frac{(\omega_2 / \omega_1) (\mathbf{q}_{2t} \cdot \mathbf{e}^*) \exp(\mathbf{q}_t \cdot \mathbf{b}/2)}{[q_{2t}^2 + \omega_1^2 / \gamma^2]} \\ & \times \int dk_3 [k_t^2 + k_3^2 / \gamma^2]^{-1} [q_{1t}^2 + (2\omega_1 - \omega_2 + k_3)^2 / \gamma^2]^{-1} [k_3 + \omega_1 - \omega_2 - k_3^2 / 2\omega_1 \gamma^2]^{-1} \end{aligned} \quad (47)$$

The corresponding cross section which is obtained from amplitudes \mathcal{M}_a and \mathcal{M}_d is given by $d\sigma_a + d\sigma_b + d\sigma_{int} = 2d\sigma_a$. The interference term $d\sigma_{int}$ yields a contribution of order of $1/\gamma^2$ after azimuthal integration, and is disregarded.

The last term in the integrand over k_3 dominates the integral in eq. 46 and it is strongly peaked (with width of order of M/γ) at $k_3 \simeq \omega_1 - \omega_2$. We can replace this value in the other terms of the integrand and take them out of the integral. The remaining integral can be done analytically. We get

$$\mathcal{M}_a = i32 (Z\alpha)^3 \frac{\Psi(0)}{M^{3/2}} \int d^2 q_t dk_t k_t \frac{(\mathbf{q}_{1t} \cdot \mathbf{e}^*) \exp(\mathbf{q}_t \cdot \mathbf{b}/2)}{[q_{1t}^2 + \omega_2^2 / \gamma^2]} \frac{1}{[k_t^2 + (\omega_1 - \omega_2)^2 / \gamma^2]} \frac{1}{[q_{2t}^2 + (2\omega_1 - \omega_2)^2 / \gamma^2]} \quad (48)$$

The same trick can be applied to the amplitude of eq. 47.

We now use eq. 16 and integrate the squared amplitude over b , multiplying by a factor of 2 to account for the amplitude of diagram (d) of figure 3. Again, we insert the nuclear form factors at each of the nuclear vertices to account for the nuclear sizes. We also change the integration variables to \mathbf{q}_{1t} and \mathbf{q}_{2t} . The final result, after integrating over $|\mathbf{q}_{1t} \cdot \hat{\mathbf{e}}^*|^2$, is

$$\frac{d\sigma}{dP_z} = 1024\pi |\Psi(0)|^2 (Z\alpha)^6 \frac{1}{M^3 E} \int \frac{dq_{1t} q_{1t}^3 [F(q_{1t}^2)]^2}{(q_{1t}^2 + \omega_2^2/\gamma^2)^2} \int \frac{dq_{2t} q_{2t} [F(q_{2t}^2)]^2}{[q_{2t}^2 + (2\omega_1 - \omega_2)^2/\gamma^2]^2} \left[\int \frac{dk_t k_t F(k_t^2)}{(k_t^2 + (\omega_1 - \omega_2)^2/\gamma^2)} \right]^2 \quad (49)$$

We now use the relationship between E and P_z to ω_1 and ω_2 and get rid of the meson wavefunction at the origin. The wavefunction $|\Psi(0)|^2$ cannot be related to the $\gamma\gamma$ decay widths. But, vector mesons can decay into e^+e^- pairs. These decay widths are very well known experimentally. Following a similar derivation as for the $\gamma\gamma$ -decay the e^+e^- decay-width of the vector mesons can be shown [23] to be equal to $\Gamma_{e^+e^-} = 16\pi\alpha^2 |\Psi(0)|^2 / 3M^2 (3 \cdot \sum_i Q_i^2)$. Inserting these results in the above equation, the factor $(3 \cdot \sum_i Q_i^2)$ will cancel out for the same reason as explained in section 3, and we get

$$\frac{d\sigma}{d\omega} = \sigma^{(-)} \frac{n(\omega)}{\omega} H(M, \omega) \quad (50)$$

where

$$\sigma^{(-)} = 96\pi \frac{\Gamma_{e^+e^-}}{M^3}, \quad (51)$$

with $n(\omega)$ given by 31 and

$$H(M, \omega) = Z^4 \alpha^3 M^2 \int \frac{dq_{2t} q_{2t} [F(q_{2t}^2)]^2}{[q_{2t}^2 + (M^2/2\omega - \omega)^2/\gamma^2]^2} \left[\int \frac{dk_t k_t F(k_t^2)}{(k_t^2 + (M^2/4\omega - \omega)^2/\gamma^2)^2} \right]^2 \quad (52)$$

The above formulas should also be valid for the production of the ortho-positronium in ultra-peripheral collisions of relativistic heavy ions. For RHIC ($Au + Au$) we obtain $\sigma = 11.2$ mb, while for the LHC ($Pb + Pb$) we get $\sigma = 35$ mb. These numbers are somewhat larger, but are in the same ballpark as the results given in ref. [17]. Note that Coulomb corrections [17] substantially modify the positronium production cross section in relativistic heavy ion collisions. This is not considered in the present approach.

In table 2 we present the cross sections for the production of vector mesons by means of the three-photon fusion process. We use the form factor given by eq. 36.

Table 2. Cross sections for three-photon production of vector ($C = odd$) mesons at RHIC ($Au + Au$) and at LHC ($Pb + Pb$).

meson	mass [MeV]	$\Gamma_{e^+e^-}$ [keV]	$\sigma^{(-)}$ [nb]	σ^{RHIC} [nb]	σ^{LHC} [nb]
ρ^0	770	6.77	1740	137	1801
ω	782	0.60	147	13	163
J/ψ	3097	5.26	21	31	423
Ψ'	3686	2.12	5	12	155

We see that the cross sections for the production of vector mesons in ultra-peripheral collisions of relativistic heavy ions are small. They do not compare to the production of vector mesons in central collisions. In principle, one would expect that the cross sections for three-photon production would scale as $(Z\alpha)^3$, which is an extra $Z\alpha$ factor compared to the two-photon fusion cross sections. However, the integral over the additional photon momentum decreases the cross section by several orders of magnitude.

V. CONCLUSIONS

We have carried out a derivation of the production of mesons in ultra-peripheral collisions of relativistic heavy ions in terms of a projection procedure. This is useful in order to study the virtuality content of the exchanged photons. We have shown that the cross section for the production of the (para-)positronium is the same as that obtained by another calculation [17].

It has also been shown that the inclusion of nuclear form factors leads to cross sections for two-photon fusion which agree with those obtained by the equivalent photon approximation. As a byproduct we extended the calculation to the production of vector mesons. We have shown that their cross sections are very small and can be neglected for practical purposes.

This work has been authored under Contract No. DE-AC02-98CH10886 with the U.S. Department of Energy, and partial support from the Brazilian funding agency MCT/FINEP/CNPQ(PRONEX), under contract No. 41.96.0886.00, is also acknowledged. One of us (CAB) is a fellow of the John Simon Guggenheim Foundation. We had also financial support from FAPESP under contract 1999/12987-5.

-
- [1] S.J. Brodsky, T. Kinoshita and H. Terazawa, Phys. Rev. Lett. **25**, 972 (1970).
 - [2] F.E. Low, Phys. Rev. **120**, 582 (1960).
 - [3] E. Fermi, Z. Phys. **29**, 315 (1924); C. F. Weizsäcker Z. Phys. **88**, 612 (1934); E.J. Williams, Phys. Rev. **45**, 729 (1934).
 - [4] G. Baur and C.A. Bertulani, Z. Phys. **A330**, 77 (1988); Phys. Rep. **163**, 299 (1988); Nucl. Phys. **A505**, 835 (1989).
 - [5] C.N. Yang, Phys. Rev. **77**, 242 (1950); L. Wolfenstein and D.G. Ravenhall, Phys. Rev. **88**, 279 (1952).
 - [6] E. Papageorgiu, Phys. Rev. **D40**, 92 (1989).
 - [7] M. Grabiak, B. Müller, W. Greiner and P. Koch, J. Phys. **G15**, L25 (1989).
 - [8] M. Drees, J. Ellis and D. Zeppenfeld, Phys. Lett. **B223**, 454 (1989).
 - [9] G. Baur and L.G. Ferreira Filho, Nucl. Phys. **A518**, 786 (1990).
 - [10] R.N. Cahn and J.D. Jackson, Phys. Rev. **D42**, 3690 (1990).
 - [11] J. Norbury, Phys. Rev. **D42**, 3696 (1990) B. Müller and A.J. Schramm, Phys. Rev. **D42**, 3699 (1990).
 - [12] A.J. Baltz and M. Strikman, Phys. Rev. **D57**, 548 (1998).
 - [13] C.G. Roldão and A.A. Natale, Phys. Rev. **C61**, 064907 (2000).
 - [14] “Heavy Ion Physics Programme in CMS”, CMS Note 2000/060, CERN, December 2000.
 - [15] G. Baur, K. Hencken and D. Trautmann, J. Phys. **G24**, 1657 (1998).
 - [16] V.A. Novikov et al., Phys. Rep. **41C**, 1 (1978).
 - [17] G.L. Kotkin, E.A. Kuraev, A. Schiller and V.G. Serbo, Phys. Rev. **D59**, 2734 (1999).
 - [18] G.T. Bodwin, D.R. Yennie and M.A. Gregorio, Rev. Mod. Phys. **57**, 723 (1985).
 - [19] C.W. de Jager, H. de Vries and C. de Vries, Atomic Data and Nuclear Data Tables **14**, 479 (1974).
 - [20] “Theory of hydrogenic bound states”, J. Sapirstein and D.R. Yennie, in “Quantum electrodynamics”, edited by T. Kinoshita, World Scientific, Singapore (1990).
 - [21] V. B. Berestetskii, E.M. Lifshitz and L.P. Pitaevskii, *Quantum Electrodynamics*, 2nd edition, Pergamon, Oxford, 1982.
 - [22] E.D. Theriot, Jr., R. H. Beers, V. W. Hughes, and K. O. H. Ziock, Phys. Rev. **A2**, 707 (1970).
 - [23] R.P. Royen and V.F. Weisskopf, Nuovo Cim. **A50**, 617 (1967).
 - [24] T. Appelquist and H.D. Politzer, Phys. Rev. Lett. **34**, 43 (1975).
 - [25] K.T.R. Davies and J.R. Nix, Phys. Rev. **C14**, 1977 (1976).
 - [26] “Symbolic Manipulation with FORM”, J.A. M. Vermaseren, CAN Publishing, The Netherherlands, 1991.